Identification of Droughts and Heat Waves in Germany with Regional Climate Networks

Gerd Schädler and Marcus Breil

Institute of Meteorology and Climate Research - Department Troposphere Research, Karlsruhe Institute of Technology, Karlsruhe, Germany

Correspondence: Gerd Schädler (gerd.schaedler@kit.edu)

Abstract.

Regional Climate Networks (RCNs) are used to identify heat waves and droughts in Germany and two subregions for the summer half years resp. summer seasons of the period 1951 to 2019. RCNs provide information for whole areas (in contrast to the point-wise information from standard indices), the underlying nodes can be distributed arbitrarily, they are easy to
5   construct and provide details otherwise difficult to avail of like extent, intensity and collective behaviour of extreme events. The RCNs were constructed on the regular 0.25 degree grid of the E-Obs data set. The season-wise correlation of time series of daily maximum temperature T_{max} and precipitation were used to construct the adjacency matrix of the networks. Metrics to identify extremes were the edge density, the 90th percentile of the correlations and the average clustering coefficient, which turned out to be highly correlated; they increased considerably during extreme events. The standard indices for comparison
10 were the effective drought and heat index (EDI and EHI) respectively, based on the same time series, and complemented by other published data. Our results show that the RCNs are able to identify severe extremes in all cases and moderate extremes in most cases. An interesting finding is that during average years, the distribution of the node degrees is close to the Poisson distribution, characteristic of random networks, while for extreme years the distribution is more uniform and heavy tailed.

1   Introduction

15 Extreme events such as heat waves, droughts and floods are causing casualities, severe damage and economic losses. It is predicted that the frequency and intensity of such extremes will increase during this century in several European regions, already affected ones such as in the Mediterranean as well as new ones in midlatitudes (Beniston et al., 2007). Knowledge about the present state and future changes of extremes is of great importance both from the scientific (process understanding) as well as from a societal standpoint (adaptation and mitigation measures) perspective. It would therefore be very useful to
20 have a fast and easy-to-apply tool to identify extremes.

To identify extreme events, several extreme indices have been developed, like the Standardised Precipitation Index (SPI) for floods, the Universal Thermal Climate Index (UTCI) for heat waves and the Palmer Drought Index (PDI) and the Effective Drought Index (EDI) for droughts, see for instance the WMO guideline for precipitation and temperature extremes (ETCCDI, http://www.wmo.int/pages/prog/wcp/wcdmp/CA_3.php). These indices are used to produce catalogues of extreme events like

the ones published by the European Drought Observatory (https://edo.jrc.ec.europa.eu/edov2/php/index.php?id=1000). However, these indices differ considerably in purpose, timescales of interest, methods used, thresholds and therefore also in events considered extreme (Byun and Wilhite, 1999).

We propose here a method to identify extreme events based on regional climate networks (RCNs) which can be applied to various types of extremes, is easy to apply, has very few tuning parameters and permits a fast analysis for whole regions instead of single points (as do most commonly used indices). The attribute "regional" means that the nodes of these networks are confined to a geographical region as opposed to the whole globe, similar to the difference between regional and global climate models; it is indeed our ultimate goal to apply the RCNs to the output of regional climate models. Extreme events happen in regions larger than a minimum size (several ten thousands of square kilometers) and are coherent and collective, i.e. most sites in such a region are affected in a similar way, so that the time series (extended over several months) of the relevant variables (daily maximum temperature, dry days) are highly correlated during extreme events. The general idea, then, of climate networks is to consider geographical points, which can be the grid points of reanalysis data, of a climate model, or a network of observation sites, as nodes of the network. A link between two nodes exists if the correlation measure (e.g. the Pearson correlation coefficient for continuous data or the Hamming distance for yes/no series) between the time series of the variables exceeds a given threshold. From this, one obtains the so-called adjacency matrix, which is essentially a list of connected nodes. Metrics of this adjacency matrix like node degree, edge density and correlation percentiles can then be used as indicators for extreme events like heat waves, floods and droughts (see e.g. Tsonis et al. (2006b)).

The study of networks has evolved from graph theory; so-called random networks have been studied mathematically by Erdös and Renyi (Erdös and Rényi (1959)). Soon they were recognised as a very useful tool to design real-world networks like electricity grids or the internet and assess their vulnerability. An overview over networks in general and their various applications in different disciplines can be found e.g. in Newman (2003), Watts and Strogatz (1998) and Albert and Barabási (2002).

Climate networks have been increasingly used in recent years, mainly in a global context. They were applied to study global oscillation patterns like El Niño and to reveal teleconnections by Donges et al. (2009) (this paper also contains definitions of higher-level network metrics). Tsonis and Swanson (2012) used climate networks to study decadal climate variability, Ludescher et al. (2013) developed a network method to improve El Niño forecasting, and Boers et al. (2014) did so for the prediction of extreme floods. It has also been shown that climate networks are able to extract interesting information about climate processes, e.g. the relation between climate and topography (Peron et al., 2014). Up to now, there are very few applications of climate networks on regional scales, although there are promising results; one of the few studies is Weimer et al. (2016), who have used a climate network to predict future heat periods in Europe on decadal time scales; they found that the network approach is in some regions and decades superior to the standard approach to estimate the occurence of heat periods. In the present study, we use RCNs to analyse the occurence of past heat and drought extremes in Germany and show that they have the potential to describe the occurence frequency, spatial extent and intensity of droughts and heat waves. This study should be considered a proof-of-concept study; our ultimate goal is to apply RCNs to projections of regional climate models

in various regions to assess future changes of extremes. From the process understanding perspective, studying the structure of the adjacency matrix permits assessing "noise" factors like orography, land use and weather patterns.

This paper is structured as follows: in section 2, we describe the construction of networks and introduce the metrics used. We also present the data and reference extreme catalogues used as well as the regions considered. In section 3, we present
5   comparisons of heat waves and drought extremes identified with RCNs with standard indices and discuss the effects of chosen regions and season. A summary is given in section 4.

2   Methods and data

2.1   Construction of RCNs and metrics used

We describe here only those aspects of climate networks which are relevant to our study; for more information on networks
10   in general, the reader is referred to e.g. Newman (2003), Watts and Strogatz (1998) or Albert and Barabási (2002); climate networks are described e.g. in Tsonis et al. (2006a) and Donges et al. (2009). We construct our RCNs, i.e. adjacency matrices, as undirected graphs with grid points of a regular lon-lat grid as nodes; two nodes are connected by an edge if the correlation of time series of the daily maximum temperatue T_{max} for heat waves resp. dry days (daily precipitation sums less than $1mm/day$) for droughts between the two nodes exceeds a predefined threshold; suitable thresholds are be determined in sensitivity studies
15   (see section 3). In order to assess the impact of the time scales on the identification of extremes, we consider heat waves and droughts occuring in the summer half year (SHY, May to October) and summer season (June to August, JJA), so that the length of the time series for each year is 184 days resp. 92 days. Although droughts are known to occur also in winter, we only consider SHY and JJA droughts here.

If we denote the number of nodes by n, the maximum possible number of edges is $\epsilon_{max} = \binom{n}{2} = n(n-1)/2$. The adjacency
20   matrix A is then an $n \times n$ matrix with $a_{ij} = 1$ if node i and node j are connected and 0 otherwise. The degree of node k, i.e. the number of nodes connected to it, will be denoted by d_k. To analyse the adjacency matrix and to identify extremes, we used the following metrics (see e.g. Newman (2003) or Donges et al. (2009)):

- the edge density ϵ, defined as the number of edges in the network, divided by ϵ_{max}; this can be considered a measure of the spatial extent of the extreme event.

25   - closely related to ϵ is p_{90}, the 90th percentile of the correlation coefficient distribution of the network. This can be considered a measure of the collective behaviour resp. intensity of the extreme event.

- the average (triangle) clustering coefficient $\bar{c}$, defined as the average of the local clustering coefficients $c_k = \Delta_k/\Delta_{max,k}$, where Δ_k is the number of triangles connected to node k and $\Delta_{max,k} = \binom{d_k}{2}$ is the number of all triangles centered at node k (see Newman (2003), Watts and Strogatz (1998)). High values of $\bar{c}$ indicate strong collective behaviour, i.e.
30   intense extreme events.

– the distribution of the node degrees d_k. For random networks, this distribution is a Poisson distribution with the average degree as parameter, being the limit of a binomial distribution (Newman, 2003); thus, deviations from the Poisson distribution can be viewed as an indicator of non-random cooperative behaviour and occurence of extremes.

We found that in the framework of this study, these metrics are sufficient to identify extremes and therefore did not consider

5   more elaborated metrics like path length, betweenness, mutual information etc. as described e.g. in (Donges et al., 2009). The time series of the yearly SHY and JJA metrics were normalised by their average and standard deviation over the period 1951 to 2019; if the metric of a period is larger than one standard deviation, this period is considered severely extreme; values within a margin around 1 (about ± 0.2) are considered moderately extreme. This margin takes into account the smoothing effect of spatial and temporal averaging on the extreme indices.

10   During average years, one would expect a network structure resembling a random network with a node degree distribution close to a Poisson distribution (Newman, 2003) due to "noise" like orography, land use and regionally changing weather conditions, resulting in values of ϵ, p_{90} and $\bar{c}$ below one standard deviation. By contrast, during extreme periods, large scale synchronous behaviour will prevail; this, together with reduced impact of noise will result in higher edge density and strong correlations between nodes and values around or above one standard deviation. This is qualitatively summarised in the following table for the normalised metrics:

normalised metric	average year	extreme year
ϵ	< 1	> 1
p_{90}	< 1	>1
$\bar{c}$	< 1	>1

Table 1. Expected normalised network metrics in average and extreme years.

15

It can also be expected that metrics will be generally lower in structured, non-uniform regions.

2.2   Data used for building the CNs

Several time series of gridded temperature and precipitation data are freely available, e.g E-Obs (Cornes et al., 2018), ERA reanalyses (Hersbach et al., 2020) and data sets from national weather services, e.g. the German Weather Service DWD;

20   differences between these data sets are due to spatial and temporal resolution, observations used and statistical/interpolation methods. A comparison of such data sets can be found in (Skok et al., 2016).

In this study, we used the E-Obs V21.0e T_{max} and precipitation gridded daily data sets (https://surfobs.climate.copernicus. eu/dataaccess/access_eobs.php). This data set has a spatial resolution of 0.25 degrees and covers the period from 1950 to 2019; it is updated continuously. The selected region was 5 to 16 degrees longitude East and 47 to 56 degrees latitude North, covering

25   Germany (see Fig. 1). We selected E-Obs for its relatively high resolution, its long time coverage and also for comparability due to its frequent use in other studies; but note that only data for land surfaces are provided by E-Obs. We focus here on Germany due to the high density of stations for interpolation and the availability of extreme event catalogues for comparison.

For the definition of edges in the heat wave case, the usual Pearson correlation coefficient was used. For droughts, from the precipitation time series a 0-1 time series of dry days was calculated as follows: if for a given day, the daily precipitation sum was less than 1 mm, this day was assigned a 1, otherwise, it was assigned a 0. Two nodes were connected if the dot product of their 0-1 series, divided by the length of the time series, exceeded a given threshold (see section 3).

5 ## 2.3 Identification of extreme events using EDI/EHI and other sources

There exist several indices to identify and to quantify the severity of extremes, like SPI, WASP index, SDI, PDI and several others for drought; they differ among each other in purpose, definition of extreme, method employed, spatial and temporal scales, focus on meteorology (precipitation) or hydrology (soil moisture, runoff); a discussion of such differences for droughts can be found in Byun and Wilhite (1999). Therefore, each choice of index is somewhat arguable and mainly owned to the need
10 for a reference.

In this study, extreme events are identified by using spatial and temporal averages of the effective drought index (EDI, Byun and Wilhite (1999)) and an analogous metric defined for heat, the effective heat index (EHI, Sedlmeier et al. (2016)), which are basically time series of effective temperature resp. precipitation, normalised by mean and standard deviation. Therefore, (relative) extremes occur when these indices deviate markedly from zero. EDI resp. EHI are easy to calculate, use a minimum
15 of assumptions, need no correction for trends and take the memory effect of the soil resp. the atmosphere into account, which is important for the assessment of the severity of heat waves and droughts. Being aware that there is no "best" index, we will at times also have a look at other extreme event indices (see section 3).

We describe here the calculation the effective drought index (EDI), the effective heat index (EHI) is calclated similarly by using T_{max} (see Sedlmeier et al. (2016)). The EDI was proposed by (Byun and Wilhite, 1999) and describes drought
20 extremes at a site as deviations from a climatological mean state; it uses the concept of effective precipitation (EP), which takes the memory effect of the soil into account. It correlates highly with soil moisture, which makes it well suited for studying droughts.

The effective precipitation EP for a given day d is calculated as follows:

$$EP(d) = \sum_{k=1}^{365} \omega_k \cdot S_k(d)$$

25 where the weights are $\omega_k = 1/k, k = 1, \cdots, 365$ and

$$S_k(d) = \sum_{i=1}^{k} P(d-i)$$

is the precipitation sum over the last k days before day d. From $EP(d)$, the (daily) $EDI(d)$ is calculated as

$$EDI(d) = (EP(d) - \overline{EP})/\sigma(EP)$$

where $\overline{EP}$ and $\sigma(EP)$ are the mean and standard deviation of EP for SHY resp. JJA over the period 1951 to 2019.

Nonlinear Processes
in Geophysics
Discussions

An analogous measure can be defined for temperature, called the effective heat index (EHI) with the daily maximum temperature T_{max} and $k = 49$ instead of $k = 365$ days. For the effective temperature, the value of 49 was determined as the lag where the autocorrelation function equals 0.5 (see Sedlmeier et al. (2016)).

One problem in connection with EDI/EHI and many other extreme indices is that they are defined at points, whereas for extremes, one is interested in area information. As mentioned in the introduction, this is one of the advantges of RCNs. For the comparison of the (area-wise) RCN metrics with the (point-wise) EDI/EHI, we calculated an area and seasonal average of the EDI from the area averaged effective precipitation and of the EHI from the area averaged effective T_{max}; to account for the smoothing of extremes due to this averaging, for a given year, season and region we define droughts as extreme when the spatially and temporally averaged EDI is less than -1, and heat events as extreme when the spatially and temporally averaged EHI is larger than +1. We are aware that there is a certain arbitrariness in this definition. We try to reduce this arbitrariness by considering also other indices when there are large differences between EDI/EHI and RCN metrics or by relaxing the threshold in cases where EDI/EHI or RCN metrics are close to the threshold.

Valuable sources of information on the occurence of extremes are Hannaford et al. (2011), Parry et al. (2012) and Spinoni et al. (2015). Hannaford et al. (2011) provide a detailed analysis, based on precipitation and runoff observations, of drought events (meteorological and hydrological) for several regions in Europe, among them subregions of Germany for the period 1961 to 2005. We will refer mainly to this dataset to complement our comparison with EDI. For heat waves, we will refer to Kornhuber et al. (2019), Vautard et al. (2007),Vautard et al. (2020), Zschenderlein et al. (2019), Russo et al. (2015) and Luterbacher et al. (2004).

3 Results

In this section, we discuss the comparison between EDI/EHI and RCN metrics in the summer half year (SHY, May till October) and summer season (JJA, June till August) for Germany (GE) and two subregions (northern Germany (GEN) and southern Germany (GES)) with respect to droughts and heat waves. EDI and EHI are averaged spatially over the respective regions. All metrics discussed below are normalised with their average and standard deviation over the period 1951 to 2019. The regions considered are shown in Fig. 1.

The choice of the correlation threshold of the time series determines the entries of the adjacency matrix, which in turn determines all metrics like node degree, correlation percentiles, clustering coefficient and other derived metrics; it is the only tuning parameter of our RCN. In a first step, we therefore conducted a series of sensitivity runs with respect to correlation threshold and its effect on the metrics. The essential criterion here is the average edge density which should be not to small in order to have enough data for calculating the metrics, but also not to large in order to have detectable differences between average and extreme years. We found that an average edge density of about 0.01 gives good results (the exact value is not important). We found no marked differences in average edge densities and resulting metrics for correlation thresholds above 0.90. We therefore chose a value of 0.95 as correlation threshold for the edges.
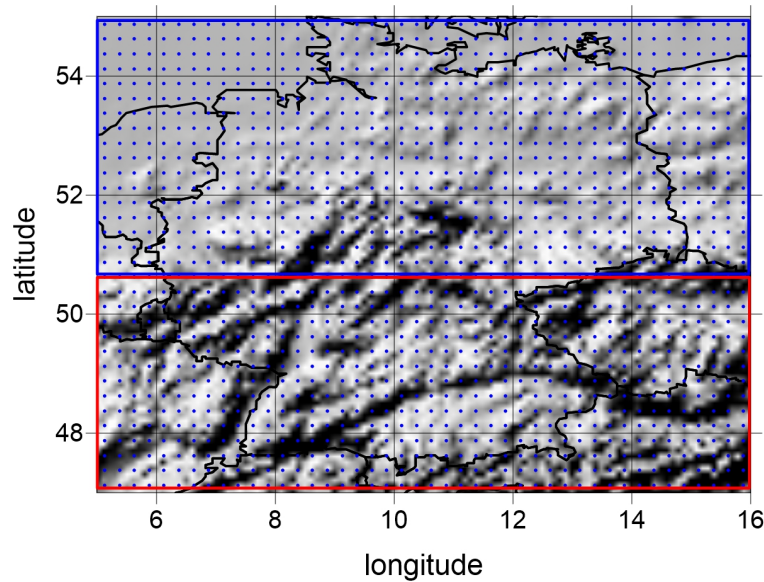
Figure 1. Germany with GES (red rectangle) and GEN (blue rectangle) subregions considered in this study. The E-Obs grid is marked by blue dots.

3.1 Droughts

3.1.1 Droughts SHY

Fig. 2 shows the time series of edge density ϵ, correlation percentile p_{90} and clustering coefficient $\bar{c}$ for the summer half years over Germany. Three years with extreme peaks close or above 2, namely 1959, 1976 and 2018, can be seen; these years are also identified as extreme by the EDI and in the literature (e.g. Spinoni et al. (2015) and Hannaford et al. (2011)). Years with values around 1 (red horizontal line in the figure) are less extreme, whereas years with values well below 1 are considered average years. The figure shows that the metrics considered are highly correlated: the Pearson correlation coefficient ρ is $\rho(\epsilon, p_{90}) =$ 0.93, $\rho(\epsilon, \bar{c}) = 0.87$, $\rho(p_{90}, \bar{c}) = 0.95$. Nevertheless, there are differences between the metrics (e.g. the year 2005) which can become important for "border cases" with metrics in a margin around 1. We will therefore present in the discussion below the edge density ϵ as well as the average clustering coefficient $\bar{c}$.

A central point of this study is the comparison between our reference drought index EDI and the RCN metrics, i.e. the edge density and the average clustering coefficient to see if they are related. Fig. 3 shows a scatterplot of EDI versus the edge density (left) and the clustering coefficient (right) of the RCN for Germany for the SHY of each year from 1951 to 2019. The important part of these figures with relation to extremes is the bottom right quadrant, since it is there where the years drier than average occur; extreme years are the ones with EDI < -1 and ϵ resp. $\bar{c}$ > 1; this is the region shaded in gray in the figure. However, since EDI as well as the RCN metrics represent temporal and spatial averages, we relax our definition of extreme and allow for a border zone with EDI <-0.8 and ϵ resp. $\bar{c}$ > 0.8. Fig. 3 shows that the years 1959,
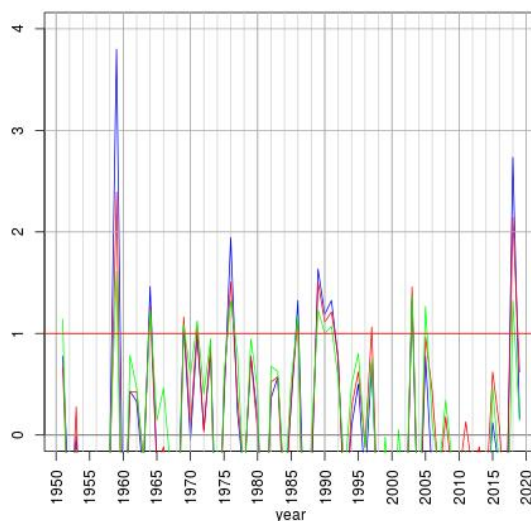
Figure 2. Time series of the SHY RCN metrics for Germany. Blue ϵ, red: p_{90}, green: $\bar{c}$.
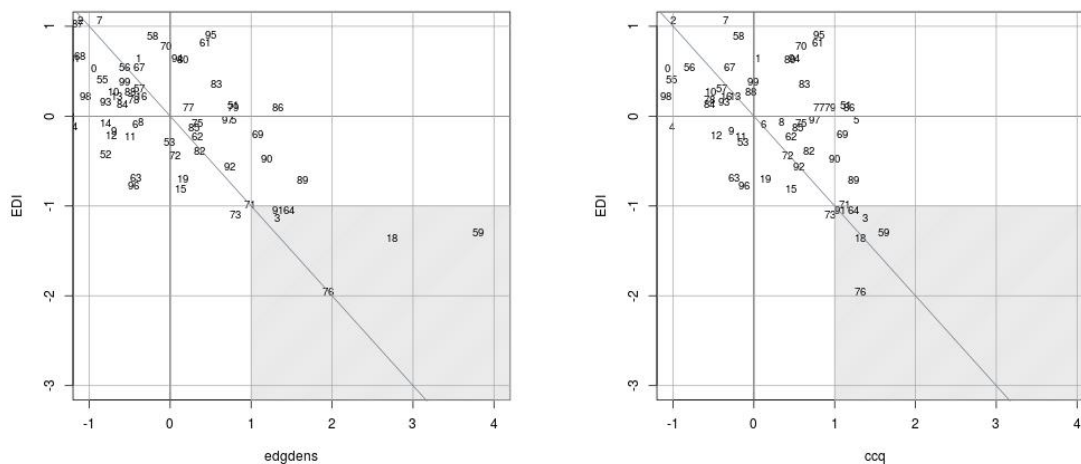

Figure 3. RCN edge density ϵ (left) and clustering coefficient $\bar{c}$ (right) vs. EDI for SHY Germany. Numbers indicate the year.

1976 and 2018 are in the gray shaded rectangle and thus are identified by the RCN and EDI as years with extreme drought, confirming the results from Fig. 2. The years 1964, 1971, 1973, 1991 and 2003 also have an EDI around 1 and also have edge density/clustering coefficient around or above 1. These years are listed as moderately to severely dry years, depending on the

source and subregion, in Hannaford et al. (2011) and Spinoni et al. (2015), and also the European Drought Reference (EDR) Database (https://www.geo.uio.no/edc/droughtdb/edr/DroughtEvents.php). This shows that the RCN is able to detect all severe SHY drought events identified by EDI and quoted in the literature. The RCN is also able to detect the less severe or only regionally severe years 1964, 1973, 1979, 1991 and 2003. There are, however, also years identified as extreme by the RCN,

5 but not by EDI. Such years are the years 1969, 1986, 1989, 1990 and 2005. These years are identified as moderately extreme in parts of Germany in Hannaford et al. (2011); this combination of weaker signal and only regional occurence could cause the difference between EDI and RCN.

3.1.2 Droughts: RCN metrics differences between average and extreme years

To illustrate the differences in the network metrics between average and extreme years, we compare the metrics for the average

10 year 1970 and the drought year 1976 as shown in Table 2; the metrics are not normalised for better comparison between the regions.

metric	GE 1970/1976	GEN 1970/1976	GES 1970/1976
ϵ	.01/.027	.03/.054	.01/.043
p_{90}	.879/.917	.919/.938	.857/.927
$\bar{c}$	.526/.611	.607/.628	.458/.618

Table 2. RCN metrics (not normalised) for the years 1970 and 1976.

The table shows that all metrics increase considerably during an extreme year, indicating increased extent of droughts and connectivity in such years. Also differences between Germany as a whole and the two subregions become evident, with the more homogeneous GEN having generally higher metrics values (and thus experiencing smaller changes) than GES which has

15 more orographical "noise" (see next section).

This stronger connectivity during extreme years (higher organisation during extreme years) becomes very evident when we compare the probability distributions of the node degrees: Fig. 4 shows these distributions for the average year 2013 and the extreme year 2018. Whereas during average years, the distribution resembles a Poisson distribution with parameter $\lambda = \overline{d_k}$ (the average node degree), which is characteristic for random networks (Newman, 2003), the distribution of the node degrees

20 in an extreme year is more uniform and has a heavy tail, i.e. a considerable number of high-degree nodes. This Poisson-like distribution during average years can be explained by the low persistence of weather systems during average years and the relatively high level of "noise" induced by the presence of complex orography and varying land use which disturb the organisation process and thus leads to lower correlations, lower clustering coefficients and lower edge densities.

The spatial distributions of the network metrics also differ considerably between average and extreme years. An example

25 is shown in Fig. 5, which shows the spatial node degree distribution for the average year 1970 (left) and the extreme year 1976 (right). In 1976, average degree, maximum degree and edge density are almost double the values of 1970. Also regional differences (cf. Table 2) become visible: in the flat northern parts of Germany, especially in the northeast with quite uniform
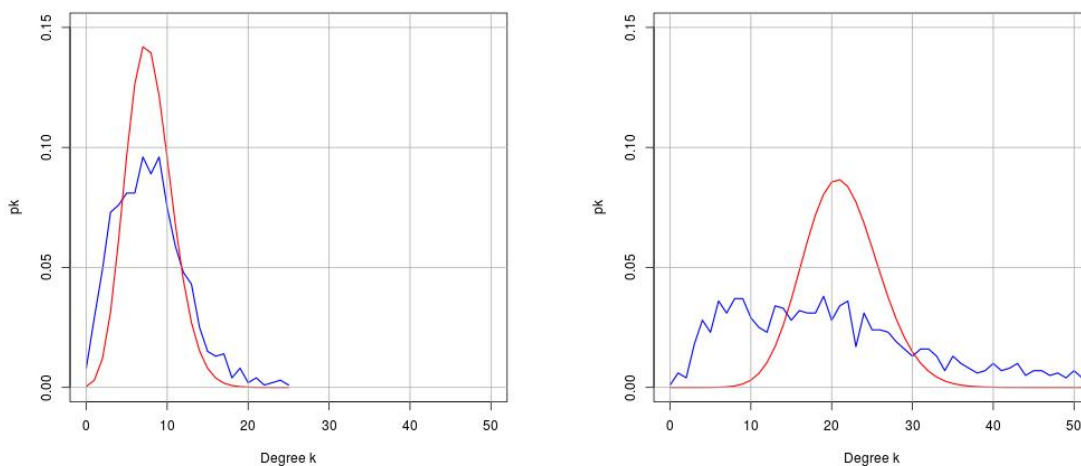
Figure 4. GE node degree probability distribution for the average year 2013 (left) and the extreme year 2018 (right).

sandy soils (reducing the precipitation recycling rate), node degrees tend to be considerably higher than in the more rugged, moutaineous and forested southern parts which favor irregular precipitation distribution and thus act as noise in the network formation. Mountaineous regions are also often the ones with lower node degree in the 1976 extreme drought year; however, exceptions occur in some mountaineous regions in the North and East, perhaps due to stronger impact of blocking highs,
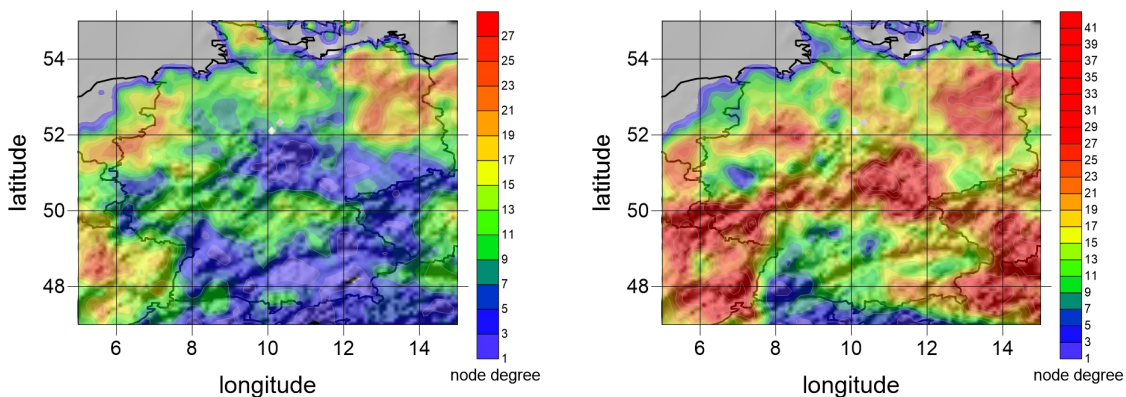5   increased continentality and less available moisture in the atmosphere.

Figure 5. Node degree distribution for the average year 1970 (left) and the extreme year 1976 (right). Note the different scales.

Nonlinear Processes
in Geophysics
Discussions

Open Access

EGU

3.1.3 Droughts: SHY extremes in GES and GEN

To illustrate the effect of orography and geographical situation, we compare the identified extreme years of the northern (GEN) part with the mountaineous southern part (GES) of Germany (see Fig. 1). Whereas GES has a complex mountaineous orography with varying land use, GEN is mostly flat, has more uniform land use with dominant sandy soils and has a more continental

5 climate. It is known that there are differences in the occurence and intensity of extreme droughts within Germany (see e.g. Samaniego et al. (2013)). Droughts can be quite regional and tend to be more frequent and more severe in the northern and northeastern parts of Germany than in the southern parts. To see if this is reflected in EDI and the RCN results, we calculated the EDI and the RCN metrics for the GES and GEN subregions. Fig. 6 shows the RCN edge density vs. EDI for GES and GEN (the plot for $\bar{c}$ is similar and is not shown).
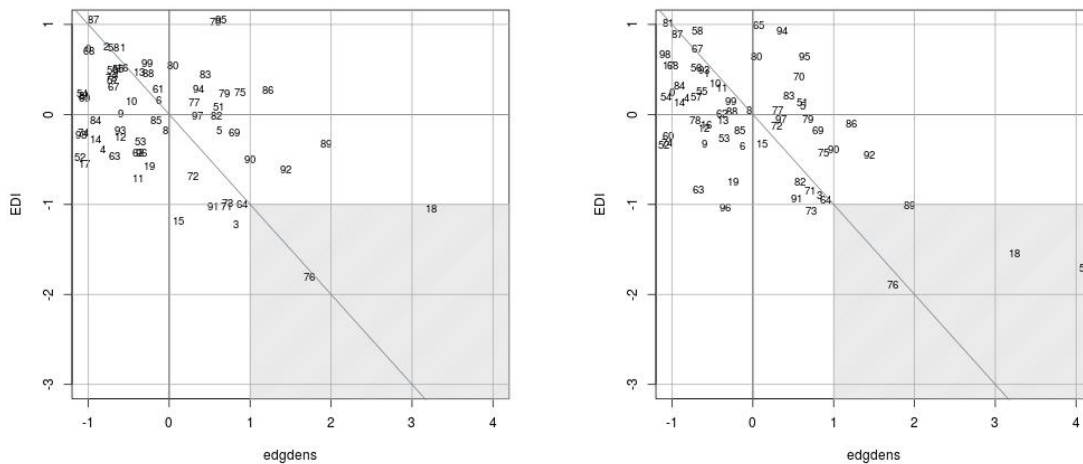

Figure 6. RCN edge density vs. EDI for GES (left) and GEN (right).

10 EDI and RCN agree in the years 1964, 1971, 1973, 1976, 1991, 2003, and 2018 as extreme years in GES. The year 2015, an extreme year in EDI, is not found by the RCN. For GEN, EDI and RCN agree in 1959, 1964, 1971, 1973, 1976, 1989, 2003 and 2018 as extreme drought years. The years 1991 and 1996, extreme years in EDI, are not identified by the RCN; it could be that the spatial extent of droughts in these years was too small to be captured by the RCN, as indicated in the maps in Samaniego et al. (2013). There are interesting differences in the occurence of extreme years between GES and GEN. For

15 example, the years 1959 and 2018, extreme years in GEN, are less extreme in GES, whereas the year 1991 is extreme in GES, but not in GEN. These regional differences, which can be seen in the maps in Samaniego et al. (2013), are well captured by the RCN and indicate that the RCN is able to identify droughts at varying spatial scales. They also illustrate the fact that the spatial scales of droughts can be down to the order of one hundred kilometers.

3.1.4 Droughts JJA

For hydrology and agriculture it is of interest to know on shorter time scales when droughts are to be expected. We therefore
compared the appearance of droughts obtained with EDI with ones obtained by the RCN for the summer (JJA) months. Figure 7
compares droughts derived from the RCN ϵ and c_{90} for JJA with the corresponding results obtained with EDI. The figure shows

5 again good agreement between EDI an RCN. The following drought years were identified by both EDI and RCN: 1959, 1964,
1973, 1976, 2003, 2015 and 2018. All years identified by EDI were also identified by the RCN. There is also good agreement
with the appearance of droughts in JJA described in Hannaford et al. (2011). Compared with the SHY drought years, the years
1971 and 1991 do not appear in JJA, probably because these droughts had their peaks in spring and autumn, whereas the years
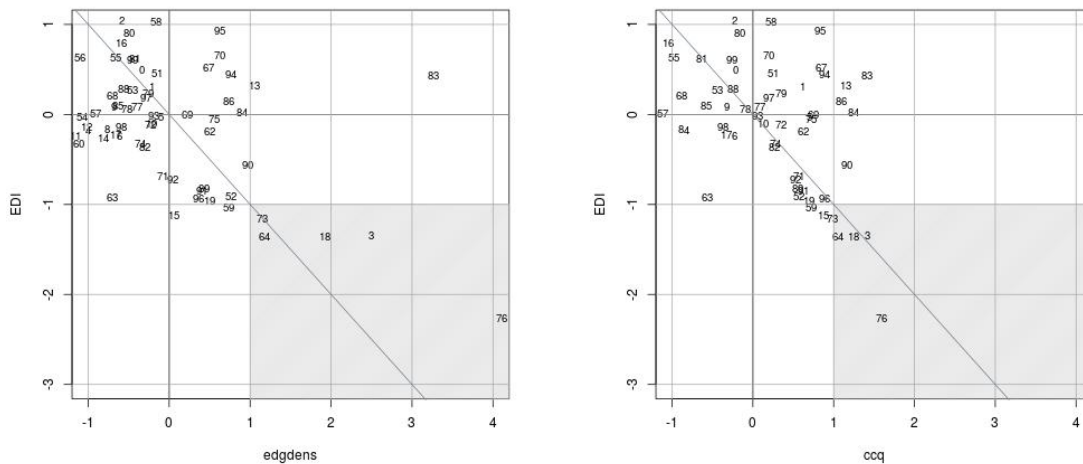2003 and 2018 are rated more severe during JJA.

Figure 7. RCN edge density (left) and clustering coefficient (right) vs. EDI for JJA Germany.

10 ## 3.2 Heat waves

In this section, we apply our RCN to heat waves and compare the RCN metrics with the EHI for Germany for the summer half
year (SHY) and the summer season (JJA), respectively.

3.2.1 Heat waves SHY

Fig. 8 shows a scatterplot of EHI versus the RCN ϵ for GE of each year from 1951 to 2019 for SHY. Similar to droughts, values

15 larger than 1 are considered as severe heat events. Since also for heat events temporal and spatial averages for EHI and RCN
are used, a margin of 0.2 is applied to account for averaging and moderate heat events, so that values above 0.8 are considered
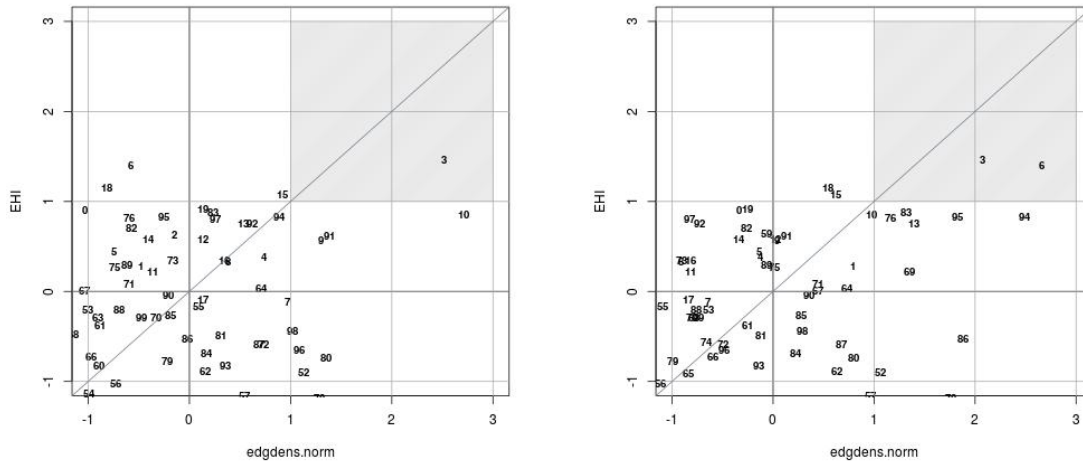
Figure 8. RCN edge density in SHY (left) and in JJA (right) vs. EDI for Germany.

as heat events. According to this definition, the years 2003 and 2006 are classified as severe heat events by the EHI, in line with literature (Luterbacher et al. (2004), Russo et al. (2015)). Additionally, the years 2014, 2015, 2016, 2018 and 2019 are identified as moderate heat events by the EHI. In literature, the years 2015, 2018 and 2019 are also mentioned as heat events in Germany (Kornhuber et al. (2019), Vautard et al. (2020)), but not the years 2014 and 2016. Moreover, in literature several

5   years are listed as heat events in Germany (1976, 1983, 1994, 1995, 2010 and 2013 (Vautard et al. (2007), Zschenderlein et al. (2019)), which are not detected in the EHI for SHY. This suggests that SHY as averaging period is too long, concealing summertime heat events.

As for the droughts, the scatterplots for the metrics largely coincide (not shown). For both network metrics, the same heat events are identified ($\rho(\epsilon, p_{90}) = 0.95$, $\rho(\epsilon, \bar{c}) = 0.96$, $\rho(\bar{c}, p_{90}) = 0.90$). The heat events in 2003 and 2015 are therefore correctly

10   identified with the network metrics. The falsely listed heat events in the years 2014 and 2016 by the EHI for SHY are not represented in the RCN. However, the heat events in 2006, 2018 and 2019 are not detected by the RCN. The missing heat events in EHI, which are listed in the literature (1976, 1983, 1994, 1995, 2010 and 2013, Vautard et al. (2007), Zschenderlein et al. (2019)), are also not captured by the RCN. The only exception is the year 2010, which is correctly classified as heat event. Furthermore, the years 1952, 1974, 1978, 1980, 1991 and 2009 are spuriously listed as heat events. Again, the averaging

15   period seems to be too long to properly detect heat events, so that neither EHI nor RCN are able to adequately identify heat events for SHY.

3.2.2   Heat waves JJA

The results of section 3.2.1 showed that the averaging period for SHY is probably too long to identify heat events in GE. For this reason, with JJA a shorter averaging period is assessed in this section. In contrast to SHY, EHI for JJA identifies four severe heat events (compared to two in SHY) for the years 2003, 2006, 2015 and 2018 (Fig. 8), in accordance with literature

5   (Kornhuber et al., 2019). Additionally, the years 1976, 1983, 1994, 1995, 2010, 2013 and 2019 are classified as moderate heat events, also in line with literature (Vautard et al. (2007), Russo et al. (2015), Zschenderlein et al. (2019), Vautard et al. (2020)). The years 1976, 1983, 1994, 1995, 2010 and 2013 are listed as heat events by EHI, while these years are not identified in SHY. The years 2014 and 2016 are not identified as heat events in JJA, while these years are falsely listed in SHY. The only year in which the EHI for JJA identifies a heat event which was not observed is 2000. This indicates that the JJA averaging period is

10   more suitable to capture spatially and temporally averaged heat events.

As in SHY, the scatterplots in JJA are highly consistent. For all network metrics, the identified heat events are identical. The years 2003 and 2006 are correctly identified as severe heat events by the RCN. However, the severe heat events in 2015 und 2018 are not reflected in the RCN metrics. Although ϵ, p_{90} and $\bar{c}$ are also for these years on a high level, the values are well below 1. The moderate heat events in 1976 and 2010 in EHI are also identified as moderate events in RCN, while the moderate

15   heat events in 1983, 1994, 1995 and 2013 are classified as severe heat events. Since the classification of severe and moderate heat events strongly depends on the subregion and/or applied heat wave indicies, this can be considered as agreement. Thus, RCNs are able to detect 8 of 11 heat events within the period 1951-2019, and for two of the three missed heat events the threshold is almost reached. The only heat event which is not identified by the RCNs is the year 2019. The RCN results for JJA are consequently in good agreement with the EHI heat events. Moreover, the falsely classified heat event in 2000 by the EHI

20   is not detected by the RCN. In comparison to droughts (section 3.1.1), the spread of the RCN results is larger. The reason for this enlarged spread is that single years are listed as heat events by the RCN (1952, 1957, 1969, 1978 and 1986), but not by the EHI and other heat wave indices.

3.2.3   Heat waves: RCN metric differences between average and extreme heat years in GE, GES and GEN

We first compare the node degree distributions between an average year (here 2002) and an extreme year (here 2003). As in

25   the case of droughts, the distributions differ considerably (Fig. 9). While the node degree distribution for average years again resembles a Poisson distribution, the distribution is flat and has a heavy tail for extreme years.

In order to investigate the impact of orography and geographical situation on extreme heat events, RCN metrics are compared for average and extreme years for the GES and GEN subregions. As average year, 1974 is chosen, as extreme year 2006. The results of this comparison are summarized in Table 3 for ϵ and p_{90}; as for the droughts (cf. Table 2), the metrics were not

30   normalised for better comparison between the regions. Both ϵ and p_{90} increase considerably in extreme years compared to average years. This means that the extent and the connectivity of the RCNs are increased in such extreme years, representing intense large-scale heat events. An increase in extent and connectivity of RCNs is especially observed in GES for extreme years, reflecting particularly the lower organisation level in average years in the mountaineous regions of southern Germany. In
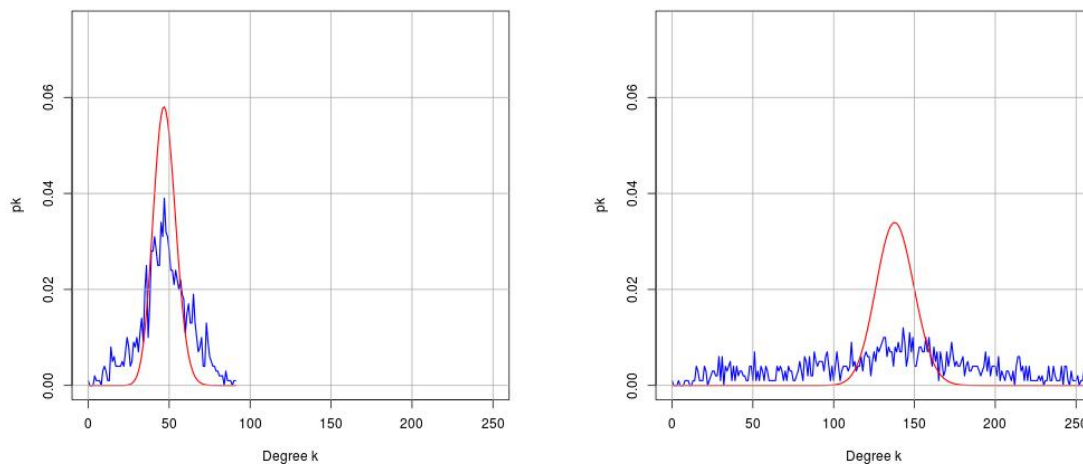
Figure 9. GE node degree probability distribution for the average year 2002 (left) and the extreme year 2003 (right).

GEN the differences between average and extreme years are less pronounced, but the metrics are generally on a higher level. This highlights the higher organisation level in the flat northern parts of Germany. These findings agree well with those for droughts in Table 2.

metric	GE	GEN	GES
ϵ	.059/.105	.126/.164	.066/.237
p_{90}	.897/.953	.987/.992	.933/.974
$\bar{c}$	.695/.729	.753/.781	.634/.701

Table 3. RCN metrics (not normalised) for the years 2002/2003.

4   Summary

5   We used Regional Climate Networks (RCNs) to identify heat waves and droughts in Germany and two subregions for the summer half years (SHY, May-October) resp. summer seasons (JJA, June-August) during the period 1951 to 2019. The RCNs were constructed from maximum daily temperature resp. precipitation data on the regular 0.25 degree grid of the EObs data set. The season-wise correlation of time series of these daily data were used to construct the adjacency matrix of the networks. Nodes were connected by an edge if the correlation of the time series was higher than 0.95. Metrics to identify extremes were

10   the edge density ϵ, the 90th percentile of the correlation distribution p_{90} and the average clustering coefficient $\bar{c}$, which turned

out to be highly correlated. The standard extreme indices for comparison were the effective drought and heat index (EDI and EHI) respectively, based on the same time series, and complemented by other published event catalogues.

Our results show that the RCNs are able to identify extremes and also to distinguish, to a certain extent, between severe and moderate events. 8 of 11 summertime heat events within the period 1951-2019 are detected by the RCNs, but also 5 false alarms; the same goes for droughts. Finding the reasons for the misses and false alarms would require a detailed analysis of

5 the regional and temporal temperature and precipitation conditions in the respective years, which is beyond the scope of the present paper.

Varying the size of the region considered showed that the occurence and intensity of extreme events found by the RCN varies with the region, in accordance with observations. Furthermore, it turned out that the applicability of RCNs to identify summertime heat events depends on the averaging period; this dependence is much less for droughts, probably due to the

10 longer time scales. All metrics increase significantly during extreme events, and probability distributions change considerably. An interesting finding is that during average years, the distribution of the node degrees resembles a Poisson distribution, characteristic of random networks, while for extreme years the distribution is more uniform and heavy tailed.

There are several advantages of RCNs over conventional methods: they provide information for whole areas (in contrast to the point-wise information from standard indices) and the extent of affected areas, they can be applied to arbitrary regions, the

15 underlying nodes can be distributed arbitrarily, they are easy to construct and they provide details otherwise difficult to avail of (e.g. regional and seasonal differences and impact of orography). An additional advantage of the method is that it is very fast. The RCN for Germany had 1338 nodes, i.e. an adjacency matrix with about 1.8 million entries; a run takes less than 4 seconds per year on a laptop, i.e. less than 5 minutes for the whole period 1951 to 2019 when written in Fortran 95. The algorithm could be accelerated further by taking advantage of the sparsity of the adjacency matrix, since only a few percent of its entries

20 are nonzero.

In this paper, we compared our RCN results with observations over the last 69 years in a year-to-year way, and we could show that the RCN approach yields useful information on extremes which can complement more conventional methods. Our ultimate goal is to use the RCN method to investigate possible future changes of the frequency and intensity of extreme events in the future. For climate model projections, one can expect that the years of occurence will vary among the models, so there

25 is no point in year-to-year comparisons. However, our present results let us expect that statistics e.g. over decades can be established reliably. One of our next goals will therefore be to apply RCNs on projections of regional climate models to assess the future development of extremes and their statistics.

From the application perspective it is interesting to use other data sets, to investigate the impact of spatial resolution, to apply the RCNs to other regions and to other extremes like floods. From the network perspective we want to analyze other network

30 metrics like cluster number and size, path lengths, mutual information and metric distributions. Also, the incorporation of other relevant information as input like soil moisture and weather patterns provide interesting insights. From a physics/climatology point of view it is important to understand in more detail why the network measures are able to represent climate dynamics and why their success varies, especially what causes misses and false alarms; this would help to improve the RCN.

Code and data availability. Codes and data will be made available within the ClimXtreme project

Appendix A

Author contributions. GS designed the study, developed computer code and performed the drought part. MB contributed the heat wave part. Both authors shared the preparation of the manuscript.

5 *Competing interests.* The authors declare that they have no conflict of interest.

References

Albert, R. and Barabási, A.-L.: Statistical mechanics of complex networks, Reviews of Modern Physics, 74, 47–97, https://doi.org/10.1103/revmodphys.74.47, http://dx.doi.org/10.1103/RevModPhys.74.47, 2002.

5 Beniston, M., Stephenson, D., Christensen, O., Ferro, C., Frei, C., Goyette, S., Halsnaes, K., Holt, T., Jylhä, K., Koffi, B., Palutikof, J., Schöll, R., Semmler, T., and Woth, K.: Future extreme events in European climate: an exploration of regional climate model projections, Climatic Change, 81, 71–95, 2007.

Boers, N., Bookhagen, B., Barbosa, H. M. J., Marwan, N., Kurths, J., and Marengo, J. A.: Prediction of extreme floods in the eastern Central Andes based on a complex networks approach, Nature Communications, 5, https://doi.org/10.1038/ncomms6199, 2014.

10 Byun, H.-R. and Wilhite, D.: Objective quantification of drought severity and duration, J. Clim., 12, 2747–2756, 1999.

Cornes, R., G., van der Schrier, E., van den Besselaar, and Jones, P.: An Ensemble Version of the E-OBS Temperature and Precipitation Datasets, J. Geophys. Res. Atmos., 123, 2747–2756, https://doi.org/10.1029/2017JD028200, 2018.

Donges, J. F., Zou, Y., Marwan, N., and Kurths, J.: Complex networks in climate dynamics, The European Physical Journal Special Topics, 174, 157–179, https://doi.org/10.1140/epjst/e2009-01098-2, http://dx.doi.org/10.1140/epjst/e2009-01098-2, 2009.

15 Erdös, P. and Rényi, A.: On Random Graphs I, Publicationes Mathematicae Debrecen, 6, 290–297, 1959.

Hannaford, J., Lloyd-Hughes, B., Keef, C., Parry, S., and Prudhomme, C.: Examining the large-scale spatial coherence of European drought using regional indicators of precipitation and streamflow deficit, Hydrological Processes, 25, 1146–1162, https://doi.org/10.1002/hyp.7725, https://onlinelibrary.wiley.com/doi/abs/10.1002/hyp.7725, 2011.

Hersbach, H., Bell, B., Berrisford, P., Hirahara, S., Horányi, A., Muñoz-Sabater, J., Nicolas, J., Peubey, C., Radu, R., Schepers, D., Sim-
20 mons, A., Soci, C., Abdalla, S., Abellan, X., Balsamo, G., Bechtold, P., Biavati, G., Bidlot, J., Bonavita, M., De Chiara, G., Dahlgren, P., Dee, D., Diamantakis, M., Dragani, R., Flemming, J., Forbes, R., Fuentes, M., Geer, A., Haimberger, L., Healy, S., Hogan, R. J., Hólm, E., Janisková, M., Keeley, S., Laloyaux, P., Lopez, P., Lupu, C., Radnoti, G., de Rosnay, P., Rozum, I., Vamborg, F., Villaume, S., and Thépaut, J.-N.: The ERA5 global reanalysis, Quarterly Journal of the Royal Meteorological Society, 146, 1999–2049, https://doi.org/https://doi.org/10.1002/qj.3803, https://rmets.onlinelibrary.wiley.com/doi/abs/10.1002/qj.3803, 2020.

25 Kornhuber, K., Osprey, S., Coumou, D., Petri, S., Petoukhov, V., Rahmstorf, S., and Gray, L.: Extreme weather events in early summer 2018 connected by a recurrent hemispheric wave-7 pattern, Environmental Research Letters, 14, 054 002, 2019.

Ludescher, J., Gozolchiani, A., Bogachev, M. I., Bunde, A., Havlin, S., and Schellnhuber, H. J.: Improved El Niño forecasting by cooperativity detection, Proceedings of the National Academy of Sciences, https://doi.org/10.1073/pnas.1309353110, http://www.pnas.org/content/early/2013/06/26/1309353110.abstract, 2013.

30 Luterbacher, J., Dietrich, D., Xoplaki, E., Grosjean, M., and Wanner, H.: European seasonal and annual temperature variability, trends, and extremes since 1500, Science, 303, 1499–1503, 2004.

Newman, M.: The Structure and Function of Complex Networks, SIAM review, 45, 167–256, https://doi.org/10.1137/S003614450342480, 2003.

Parry, S., Hannaford, J., Lloyd-Hughes, B., and Prudhomme, C.: Multi-year droughts in Europe: analysis of development and causes, Hy-
35 drology Research, 43, 689–706, https://doi.org/10.2166/nh.2012.024, https://doi.org/10.2166/nh.2012.024, 2012.

Peron, T. K. D., Comin, C. H., Amancio, D. R., da F. Costa, L., Rodrigues, F. A., and Kurths, J.: Correlations between climate network and relief data, Nonlinear Processes in Geophysics, 21, 1127–1132, https://doi.org/10.5194/npg-21-1127-2014, http://www.nonlin-processes-geophys.net/21/1127/2014/, 2014.

Russo, S., Sillmann, J., and Fischer, E. M.: Top ten European heatwaves since 1950 and their occurrence in the coming decades, Environmental Research Letters, 10, 124 003, 2015.

Samaniego, L., Kumar, R., and Zink, M.: Implications of Parameter Uncertainty on Soil Moisture Drought Analysis in Germany, Journal of
5   Hydrometeorology, 14, 47–68, https://doi.org/10.1175/JHM-D-12-075.1, https://doi.org/10.1175/JHM-D-12-075.1, 2013.

Sedlmeier, K., Mieruch, S., Schädler, G., and Kottmeier, C.: Compound extremes in a changing climate – a Markov chain approach, Nonlinear Processes in Geophysics, 23, 375–390, https://doi.org/10.5194/npg-23-375-2016, https://npg.copernicus.org/articles/23/375/2016/, 2016.

Skok, G., Žagar, N., Honzak, L., Žabkar, R., Rakovec, J., and Ceglar, A.: Precipitation intercomparison of a set of satellite- and raingauge-derived datasets, ERA Interim reanalysis, and a single WRF regional climate simulation over Europe and the North Atlantic, Theoretical
10   and Applied Climatology, 123, 217–232, 2016.

Spinoni, J., Naumann, G., Vogt, J. V., and Barbosa, P.: The biggest drought events in Europe from 1950 to 2012, Journal of Hydrology: Regional Studies, 3, 509–524, https://doi.org/10.1016/j.ejrh.2015.01.001, http://www.sciencedirect.com/science/article/pii/S2214581815000026, 2015.

Tsonis, A. A. and Swanson, K. L.: Review article "On the origins of decadal climate variability: a network perspective", Nonlinear Processes
15   in Geophysics, 19, 559–568, https://doi.org/10.5194/npg-19-559-2012, http://www.nonlin-processes-geophys.net/19/559/2012/, 2012.

Tsonis, A. A., Swanson, K., and Roebber, P. J.: What do networks have to do with climate?, Bull. Amer. Meteor. Soc., 87, 585–595, 2006a.

Tsonis, A. A., Swanson, K. L., and Roebber, P. J.: What Do Networks Have to Do with Climate?, Bulletin of the American Meteorological Society, 87, 585–596, https://doi.org/10.1175/BAMS-87-5-585, https://doi.org/10.1175/BAMS-87-5-585, 2006b.

Vautard, R., Yiou, P., D'andrea, F., De Noblet, N., Viovy, N., Cassou, C., Polcher, J., Ciais, P., Kageyama, M., and Fan, Y.: Summertime
20   European heat and drought waves induced by wintertime Mediterranean rainfall deficit, Geophysical Research Letters, 34, 2007.

Vautard, R., van Aalst, M., Boucher, O., Drouin, A., Haustein, K., Kreienkamp, F., van Oldenborgh, G. J., Otto, F. E., Ribes, A., Robin, Y., et al.: Human contribution to the record-breaking June and July 2019 heatwaves in Western Europe, Environmental Research Letters, 15, 094 077, 2020.

Watts, D. and Strogatz, S.: Collective dynamics of 'small-world' networks, Nature, pp. 440–442, 1998.

25 Weimer, M., Mieruch, S., Schädler, G., and Kottmeier, C.: A new estimator of heat periods for decadal climate predictions – a complex network approach, Nonlinear Processes in Geophysics, 23, 307–317, https://doi.org/10.5194/npg-23-307-2016, https://npg.copernicus.org/articles/23/307/2016/, 2016.

Zschenderlein, P., Fink, A. H., Pfahl, S., and Wernli, H.: Processes determining heat waves across different European climates, Quarterly Journal of the Royal Meteorological Society, 145, 2973–2989, 2019.